Biochemical and Biophysical Research Communications 434 (2013) 516–520

Contents lists available at SciVerse ScienceDirect

Biochemical and Biophysical Research Communications

journal homepage: www.elsevier.com/locate/ybbrc

DNA duplex-supported artificial esterase mimicking by cooperative grafting functional groups

Liang Xu [1], Chuanshi Ji [1], Yu Bai, Junlin He *, Keliang Liu *

Beijing Institute of Pharmacology and Toxicology, 27 Taiping Road, Beijing 100850, China

ARTICLE INFO

Article history:
Received 9 March 2013
Available online 10 April 2013

Keywords:
DNA duplex
Artificial esterase mimics
Imidazolyl group

ABSTRACT

The molecular structures of enzyme mimics may be modified to optimize their catalytic properties. In this study, to generate artificial enzyme mimics, Watson–Crick base paired DNA duplexes were designed as scaffolds which were assembled by nucleotides modified with specific functional groups. This process allowed various functional groups to be precisely assembled at different sites on the duplexes. By using this strategy, the 5-[2-(1H-imidazolyl-4)-(*E*)-ethylene]-2′-deoxythymidine (**1**) analog with the 5-substituted imidazolyl group was incorporated into single strands of DNA. Upon DNA duplex formation, several combinations of the imidazolyl group were formed. Using p-nitrophenyl acetate as the substrate of the catalytic reaction, we evaluated the hydrolysis capabilities of the imidazolyl assemblies. The catalytic ability was closely related to the distribution of imidazolyl groups in the DNA duplex. The most effective catalytic center was that of the duplex **O5**–**O6** construct with three imidazolyl groups. This construct displayed bell-shaped pH-dependent and Mg^{2+}-independent kinetic curves, which are typical characteristics of imidazolyl-mediated catalytic reactions.

1. Introduction

The design and synthesis of artificial enzymes are important challenges in the field of enzyme research. Researchers have explored the possible use of skeleton molecules, including small molecules [1–3], metal complexes [3–11], cyclodextrin [12–15], polyamines [16,17], dendrimers [18], peptides [19,20], and oligonucleotides [21–25], to support combinations of amino, imino, guanidinyl, and/or imidazolyl functional groups. These functional groups are arranged depending on the catalytic center of the particular enzyme being mimicked [26]. The imidazolyl group has been frequently applied in enzyme-mimicking studies. In particular, it has been used to construct superoxide enzyme [27], nuclease [28–32], and serine proteinase mimics [33]. Imidazolyl displays a near-neutral pK_a, enabling it to function as either a proton-donor or proton-acceptor in proton-transfer reactions. However, no any mimic has been able to replicate the precise catalytic properties of an enzyme so far. Moreover, the construction of functional group combinations has been limited by the skeleton molecules themselves.

We have developed a strategy to design enzyme mimics by using polymeric materials with definite tertiary structures as the skeleton molecules. The most attractive candidate materials are finely ordered complexes of peptides or oligonucleotides, because their components can be used as building blocks for various functional groups. The designed molecular assemblies can be conveniently formed so that all of the functional groups are precisely located, allowing the exploration of the specific functions of the assemblies. We have used the six-helix bundle (6HB) peptide to support the imidazolyl group combination through the site-specific introduction of histidines, which conduct the enzyme-like hydrolytic activity towards p-nitrophenyl acetate (PNPA) [34].

In this paper, we report the use of oligodeoxynucleotides (ODNs) as skeleton molecules. Because ODNs form specific and rigid tertiary structures, by incorporating modified residues into the ODNs, we were able to create differentially distributed functional groups in the tertiary structures [33,35]. Using this method, we obtained several combinations of imidazolyl groups in the DNA duplex **O1**–**O2**, namely, 5′-d(CGG CCT TAT CGC GC)-3′ (**O1**) paired with 3′-d(GCC GGA ATA GCG CG)-5′ (**O2**) modified with nucleoside analog 1 (Fig. 1) at various designed sites. We evaluated the hydrolytic activities of these enzyme mimics on the ester bond of PNPA.

2. Materials and methods

2.1. ODNs

All of the ODNs used in this study were synthesized on an ABI 392 nucleic acid synthesizer (Applied Biosystems, USA) at a 1-μmol scale, according to the dimethoxytrityl (DMT)-off

* Corresponding authors. Fax: +86 10 68211656.
E-mail addresses: Junlin_he@yahoo.com (J. He), keliangliu55@126.com (K. Liu).
[1] The first two authors equally contributed to this work.

0006-291X/$ - see front matter © 2013 Elsevier Inc. All rights reserved.
http://dx.doi.org/10.1016/j.bbrc.2013.03.106

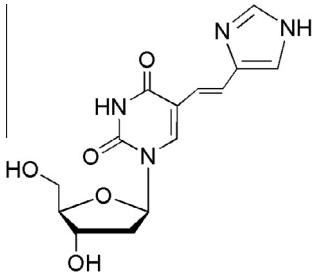

Fig. 1. Compound **1** as the replacement of 2′-deoxythymidine in the DNA duplexes.

phosphoramidite chemistry protocol (the preparation procedure of phosphoramidite of compound **1** is provided as Supplementary material). The ODNs were cleaved and deprotected by heating them with concentrated aqueous (conc. aq.) ammonia at 55 °C for 18 h. Purification was performed by reverse-phase high-performance liquid chromatography with the following solvent gradient series: [A: 0.07 M (Et_3NH)OAc (pH 7.0)/MeCN 95:5; B: MeCN]: 0–2 min, 2% B in A, 2–12 min, 2–16% B in A, at a flow rate of 1.0 mL/min. Desalting was performed on a SEP-PAK column (300 Å/360 mg; Waters, USA). The product was lyophilized and characterized by matrix-assisted laser desorption/ionization time-of-flight mass spectrometry (Supplementary Table S1) performed on a Kratos Axima-CFR™-plus mass spectrophotometer (Shimatzu, Japan) with 2′,4′,6′-trihydroxyacetophenone (THAP) as the matrix.

2.2. Kinetics measurement

The hydrolysis reaction with PNPA substrate was conducted in 96-well plates (Costar, USA) and monitored by detecting increases in absorbance (at 405/320 nm) corresponding to the release of 4-nitrophenolate with a spectra M5 spectrophotometer (Molecular Devices, USA). The absorbance spectra were selected by the maximal absorbance of p-nitrophenol occurred at 320 nm (for pH < 6) or 405 nm (for pH > 6). The 96-well plates were thermo-sealed to avoid evaporation during the measurements. The following buffers were used as reference solutions (each at 50 mM): NaOAc (pH 4.0, 4.5, 5.0), MES (pH 5.5, 6.0, 6.5), HEPES (pH 6.75, 7.0, 7.5, 8.0, 8.5), and sodium borate (pH 9.0, 9.5).

The rate of hydrolysis of PNPA by the duplexes in Table 2 was determined under the conditions of 20 μM duplex and 150 μM PNPA. One equivalent of EDTA (relative to the duplex concentration) was added to exclude the effect of the divalent metal ions. Because of the poor solubility of PNPA in water, the stock solution was prepared in acetonitrile and diluted into the buffer. The maximal acetonitrile concentration in the final reaction mixture was 2%. Buffer alone was used as the negative control (Control 1), and buffer containing 60 μM imidazole alone was used as the positive control (Control 2).

For each duplex measurement, the absorbance was plotted against time. The points were then adjusted by linear regression with the OriginPro 7.5 software package. The value of the slope was divided by the extinction coefficient to determine the hydrolysis rate for the particular duplex. The background hydrolysis rate of PNPA (150 μM) in buffer was defined as v_{uncata}. The rate enhancement (v_{net}) of each duplex was calculated as the observed reaction rate (v_{obs}) minus the v_{uncata}. To obtain the second-order rate constant (k_2), the background reaction was subtracted from the measured pseudo-first-order rate and divided by the initial concentration of catalyst (E_0) and substrate (S_0). Each data point represented the average of triplicate experiments run in parallel. The error limits were estimated to be in the range of ±10%.

Saturation kinetics experiments were performed in a reaction buffer solution (50 mM HEPES and 50 mM $MgCl_2$, pH 7.2) at 25 °C with 15 μM of duplex **O5**–**O6** and various concentrations of PNPA (50, 100, 200, 500, 1000, and 2000 μM). Three batches of duplex **O5**–**O6** had essentially identical activities (±10%). Initial velocities calculated from the linear portion of the absorbance slope at 405 nm (<5% of substrate consumed) were plotted against S_0 to obtain the Michaelis–Menten plot, by using a standard fit with the following equation:

$$v_{net} = k_{cat}[E_0][S_0]/([S_0] + K_m).$$

Table 1
T_m of DNA duplexes measured under reaction conditions[a].

Name	Duplex	T_m (°C)
O1–**O2**	5′-d(GCG CGA TAA GGC CG)-3′ 3′-d(CGC GCT ATT CCG GC)-5′	68.8
O1–**O3**	5′-d(GCG CGA TAA GGC CG)-3′ 3′-d(CGC GCT A**1**T CCG GC)-5′	67.8
O1–**O4**	5′-d(GCG CGA TAA GGC CG)-3′ 3′-d(CGC GC**1** ATT CCG GC)-5′	66.9
O5–**O2**	5′-d(GCG CGA **1**AA GGC CG)-3′ 3′-d(CGC GCT ATT CCG GC)-5′	67.0
O1–**O6**	5′-d(GCG CGA TAA GGC CG)-3′ 3′-d(CGC GC**1** A**1**T CCG GC)-5′	66.0
O5–**O3**	5′-d(GCG CGA **1**AA GGC CG)-3′ 3′-d(CGC GCT A**1**T CCG GC)-5′	66.0
O5–**O4**	5′-d(GCG CGA **1**AA GGC CG)-3′ 3′-d(CGC GC**1** ATT CCG GC)-5′	65.8
O5–**O6**	5′-d(GCG CGA **1**AA GGC CG)-3′ 3′-d(CGC GC**1** A**1**T CCG GC)-5’	62.0
O5–**O7**	5′-d(GCG CGA **1**AA GGC CG)-3′ 3′-d(CGC GCT A**11** CCG GC)-5′	62.2

[a] Measured in the reaction buffer with 5 μM ODN.

Table 2
The v_{obs} and k_2 values of PNPA hydrolysis mediated by different assemblies of imidazolyl groups in the DNA duplexes[a].

Name	Sequence	v_{obs} (M^{-1} S^{-1})	k_2 (M^{-1} S^{-1})
Control 1[b]	PNPA alone in buffer	6.78E−10	–
Control 2[c]	Imidazole and PNPA	1.43E−09	8.39E−02
O1–**O2**	5′-d(GCG CGA TAA GGC CG)-3′ 3′-d(CGC GCT ATT CCG GC)-5′	8.50E−10	5.72E−02
O1–**O3**	5′-d(GCG CGA TAA GGC CG)-3′ 3′-d(CGC GCT A**1**T CCG GC)-5′	8.28E−10	5.00E−02
O1–**O4**	5′-d(GCG CGA TAA GGC CG)-3′ 3′-d(CGC GC**1** ATT CCG GC)-5′	8.77E−10	5.66E−02
O5–**O2**	5′-d(GCG CGA **1**AA GGC CG)-3′ 3′-d(CGC GCT ATT CCG GC)-5′	8.93E−10	7.18E−02
O1–**O6**	5′-d(GCG CGA TAA GGC CG)-3′ 3′-d(CGC GC**1** A**1**T CCG GC)-5′	2.04E−09	4.55E-01
O5–**O3**	5′-d(GCG CGA **1**AA GGC CG)-3′ 3′-d(CGC GCT A**1**T CCG GC)-5′	1.39E−09	2.37E−01
O5–**O4**	5′-d(GCG CGA **1**AA GGC CG)-3′ 3′-d(CGC GC**1** ATT CCG GC)-5′	1.44E−09	2.55E−01
O5–**O6**	5′-d(GCG CGA **1**AA GGC CG)-3′ 3′-d(CGC GC**1** A**1**T CCG GC)-5′	2.49E−09	6.04E−01
O5–**O7**	5′-d(GCG CGA **1**AA GGC CG)-3′ 3′-d(CGC GCT A**11** CCG GC)-5′	1.39E−09	2.41E−01

[a] 150 μM PNPA substrate and 20 μM duplex were mixed in the reaction buffer and reacted at 25 °C.
[b] Only PNPA was added to the buffer.
[c] 60 μM imidazole was used in lieu of the DNA duplex.

3. Results and discussion

By using the oligos **O1** and **O2** together with the modified sequences **O3**–**O7**, eight different modified DNA duplexes were formed, as evidenced by their T_m values (Table 1). The T_m values of the DNA duplexes were all much higher than 25 °C (i.e., the catalytic reaction temperature). This observation indicates that the DNA duplex was the main component in the reaction mixture. Thus, a stable DNA duplex as the skeleton molecule of the

imidazolyl group assemblies had been achieved under the catalytic reaction conditions.

3.1. Hydrolytic activity of the modified DNA duplexes with various assemblies of imidazolyl groups

As shown in Table 2, the modified duplexes **O1**–**O3**, **O1**–**O4**, and **O5**–**O2** that harbored only one imidazolyl group each exhibited cleavage rates that were similar to those of the unmodified duplex **O1**–**O2**. This finding may indicate that the only one imidazolyl group from each duplex appeared to be ineffective, due to lack of imidazolyl group cooperation between the duplexes. In contrast, the duplexes with two imidazolyl groups combined, **O1**–**O6**, **O5**–**O3**, and **O5**–**O4**, showed faster rates of PNPA cleavage. This observation may indicate that two imidazolyl groups within a duplex interacted in a cooperative manner, promoting the effective catalytic hydrolysis of PNPA. It is reasonable that different combinations should yield different rates of catalytic enhancement. Motif **1**A**1** in duplex **O1**–**O6** ($k_2 = 0.455\ M^{-1}S^{-1}$) seemed to be more appropriately positioned for function in the duplex context. However, the single sequence of **O6** with motif **1**A**1** showed less-efficient hydrolysis under the same conditions ($k_2 = 0.367\ M^{-1}S^{-1}$). This result indicates that the two imidazolyl groups in a duplex or in a single stranded ODN are in totally different conformation and cooperative state. The spacial distributions and relatively fixed positions of the imidazolyl groups brought by the rigid tertiary structure of duplex can affect the cooperative efficiencies.

The two duplexes with three imidazolyl groups assembled in the duplexes, namely **O5**–**O6** and **O5**–**O7**, also mediated the catalytic hydrolysis of PNPA (Table 2). However, duplex **O5**–**O6** demonstrated a much faster reaction time compared to duplex **O5**–**O7**. Thus, the two-imidazolyl group combination defined by **1**A**1** (as occurred in both **O1**–**O6** and **O5**–**O6**) appears to be an effective motif for the future design of catalytic centers.

The hydrolytic rates of the duplexes containing two or three imidazolyl groups were enhanced compared to the rates of the free imidazole solutions. This finding further confirms that the imidazolyl groups cooperate within the duplex context. Such cooperative activities have been observed in other artificial enzyme systems with imidazolyl groups.

3.2. Kinetic characterization of duplex O5–O6

Under multiple-turnover conditions, the rate of PNPA hydrolysis by duplex **O5**–**O6** was determined over a range of substrate concentrations with steady-state kinetics treatment (Fig. 2). Hofstee analysis of the data gave a K_m value of 618.2 μM and a k_{cat} value of $3.91 \times 10^{-4}\ S^{-1}$. These findings suggest Michaelis–Menten behavior for this duplex. The k_{cat} value of duplex **O5**–**O6** indicate that the catalyzed reaction was 123-fold more efficient than background hydrolysis ($k_{uncat} = 3.19 \times 10^{-6}\ S^{-1}$). In addition, the k_{cat}/K_m value ($6.32 \times 10^{-7}\ \mu M^{-1}S^{-1}$) was 6.3-fold higher than that of the imidazole solution ($1.00 \times 10^{-7}\ \mu M^{-1}S^{-1}$). These data indicate that duplex **O5**–**O6** mediated the effective catalytic hydrolysis of PNPA.

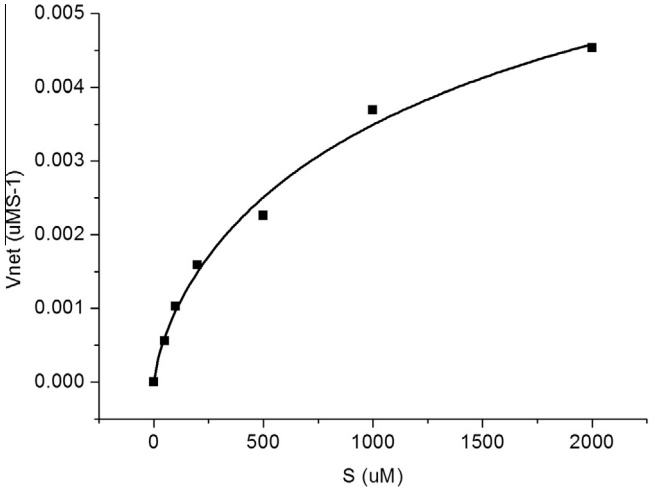

Fig. 2. Reaction rate of duplex **O5**–**O6** *vs.* concentrations of the substrate (S) PNPA.

Conformational changes in the DNA helix are reversible, unlike those of many protein enzymes. Therefore, we investigated whether the catalytic center could be recovered. When duplex **O5**–**O6** that had been reacted with PNPA was extracted from the original reaction buffer and re-incubated with fresh PNPA, the duplex continued to show catalytic behavior (Supplementary Fig. S1). Therefore, the catalytic center based on the DNA helix was recoverable.

3.3. Effect of divalent metal ion Mg^{2+} on the catalytic capability of duplex *O5*–*O6*

Mg^{2+} is an important factor for many protein and nucleic acid enzymes, playing both structural and mechanistic roles. In the present system, Mg^{2+} was used to stabilize the DNA duplexes, but we wondered whether it was also involved in the hydrolytic reaction. We observed that the duplex **O5**–**O6** mediated the catalytic hydrolysis of PNPA in the absence of Mg^{2+}, although the rate of hydrolysis was slightly slower than the rate under conditions with Mg^{2+} (Supplementary Fig. S2). This phenomenon further demonstrates that the imidazolyl group combination in duplex **O5**–**O6** was responsible for the catalytic hydrolysis. The slightly faster rate of **O5**–**O6** in the presence of Mg^{2+} suggests that Mg^{2+} affected but was not absolutely necessary for the catalytic activity of the duplex. We speculate that Mg^{2+} may contribute to the reaction by increasing the helix-binding stability of certain duplexes, specifically those in which the imidazolyl groups show an effective spatial distribution.

3.4. Effect of pH on the reaction of duplex O5–O6

Both imidazolyl and imidazolium are required for the proton transfer during imidazolyl-catalyzed hydrolysis. Thus, imidazolyl-catalyzed hydrolysis is characterized kinetically by a bell-shaped pH-dependent curve. As shown in Fig. 3, the duplex **O5**–**O6** produced the characteristic bell-shaped curve for pH, with an optimum pH range of 6.5–7.0. This finding indicates that at least two imidazolyl groups were cooperatively located within the duplex **O5**–**O6**, such that the existence of both basic imidazolyl and protonated imidazolium facilitated the proton transfer. When the pH-modulated equilibrium reached its maximum level, the reaction was greatly enhanced.

3.5. Molecular modeling of the spatial distribution of the imidazolyl groups of duplex O5–O6

The molecular structures of the duplexes **O5**–**O6** and **O5**–**O7** were determined computationally to gain insight into the relationship between the spatial distributions of the imidazolyl groups and their catalytic behaviors (for molecular dynamics calculation methods, see Supplementary materials) [36].

As shown in Fig. 4, the modeling results indicated the integrity of the DNA duplex conformation for both **O5**–**O6** and **O5**–**O7**. In each duplex, the imidazolyl group assemblies were located in the major groove. The moderate freedom of the ethenyl linkage is expected to permit a limited scope of movement for the imidazolyl group. Based on these observations, the spatial distribution of the functional group assemblies could be further manipulated (e.g.,

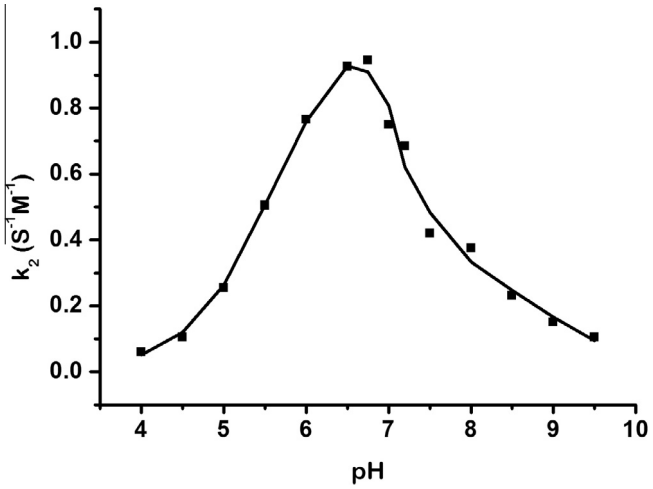

Fig. 3. pH dependence of the second-order rate constant k_2 for duplex **O5–O6** during hydrolysis of PNPA.

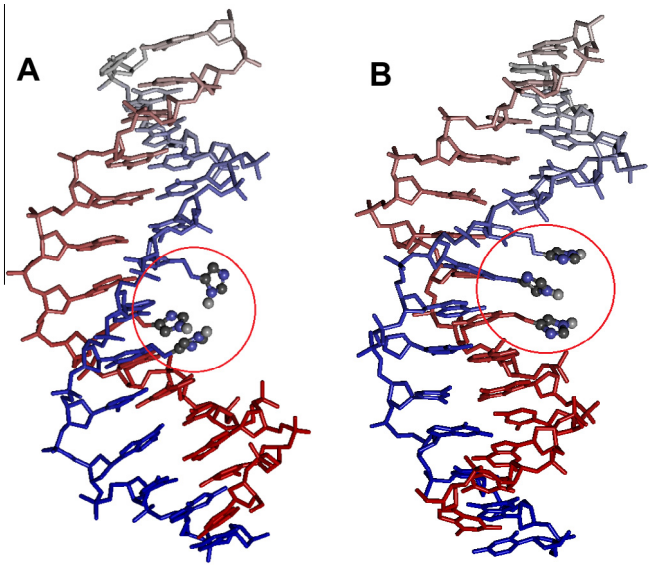

Fig. 4. Molecular structures of duplexes **O5–O6** (A) and **O5–O7** (B).

by the positioning of the modified residues or linkages of the functional groups) to achieve an even closer representation of the catalytic center of the natural enzyme.

The use of DNA duplexes as skeleton molecules allows for the convenient generation of flexible imidazolyl group assemblies. With this approach, both the number of modified residues and their positions within the ODNs may be specified. In this study, we generated eight imidazolyl group assemblies. Of the duplexes that were studied, the duplex **O5–O6** demonstrated the best hydrolysis of PNPA and a pH-dependent kinetics profile, similar to that of other imidazolyl-containing catalytic centers. Future studies will focus on optimizing the geometric structure of the imidazolyl group in this duplex. Our findings indicate that modified ODNs with various functional groups and tertiary DNA structures are feasible sources for generating functional group combinations with specific functions. In addition, this strategy may be developed for applications other than artificial enzymes.

Acknowledgments

This work was supported in part by grants from the National Natural Science Foundation of China [21102177], National Science and Technology Major Project of China [2012ZX09301003], and Natural Science Foundation of Beijing [7132154, 7123223].

Appendix A. Supplementary data

Supplementary data associated with this article can be found, in the online version, at http://dx.doi.org/10.1016/j.bbrc.2013.03.106.

References

[1] N. Kovalev, E. Burakova, V. Silnikov, M. Zenkova, V. Vlassov, Artificial ribonucleases: from combinatorial libraries to efficient catalysts of RNA cleavage, Bioorg. Chem. 34 (2006) 274–286.
[2] N.A. Kovalev, D.A. Medvedeva, M.A. Zenkova, V.V. Vlassov, Cleavage of RNA by an amphiphilic compound lacking traditional catalytic groups, Bioorg. Chem. 36 (2008) 33–45.
[3] R. Salvio, R. Cacciapaglia, L. Mandolini, General base-guanidinium cooperation in bifunctional artificial phosphodiesterases, J. Org. Chem. 76 (2011) 5438–5443.
[4] M.Y. Yang, J.P. Richard, J.R. Morrow, Substrate specificity for catalysis of phosphodiester cleavage by a dinuclear Zn(II) complex, Chem. Commun. 22 (2003) 2832–2833.
[5] J.R. Morrow, O. Iranzo, Synthetic metallonucleases for RNA cleavage, Curr. Opin. Chem. Biol. 8 (2004) 192–200.
[6] C. Liu, M. Wang, T. Zhang, H. Sun, DNA hydrolysis promoted by di- and multinuclear metal complexes, Coord. Chem. Rev. 248 (2004) 147–168.
[7] T. Gunnlaugsson, R.J.H. Davies, M. Nieuwenhuyzen, C.S. Stevenson, R. Viguier, S. Mulready, Rapid hydrolytic cleavage of the mRNA model compound HPNP by glycine based macrocyclic lanthanide ribonuclease mimics, Chem. Commun. 18 (2002) 2136–2137.
[8] M. Leivers, R. Breslow, Concerning two-metal cooperativity in model phosphate hydrolysis, Bioorg. Chem. 29 (2001) 345–356.
[9] J. Suh, W.S. Chei, Metal complexes as artificial proteases: toward catalytic drugs, Curr. Opin. Chem. Biol. 12 (2008) 207–213.
[10] N. Gao, H. Li, Q. Li, J. Liu, G. Luo, Synthesis and kinetic evaluation of a trifunctional enzyme mimic with a dimanganese active centre, J. Inorg. Biochem. 105 (2011) 283–288.
[11] A. Singh, S. Patra, J.A. Lee, K.H. Park, H. Yang, An artificial enzyme-based assay: DNA detection using a peroxidase-like copper–creatinine complex, Biosens. Bioelectron. 26 (2011) 4798–4803.
[12] R. Kataky, E. Morgan, Potential of enzyme mimics in biomimetic sensors: a modified-cyclodextrin as a dehydrogenase enzyme mimic, Biosens. Bioelectron. 18 (2003) 1407–1417.
[13] R. Breslow, Biomimetic chemistry and artificial enzymes: catalysis by design, Acc. Chem. Res. 28 (1995) 146–153.
[14] E. Lindbäck, Y. Zhou, C.M. Pedersen, M. Bols, Two diastereomeric artificial enzymes with different catalytic activity, Eur. J. Org. Chem. 27 (2012) 5366–5372.
[15] E. Lindbäck, Y. Zhou, C.M. Pedersen, M. Bols, Artificial enzymes based on cyclodextrin with phenol as the catalytic group, Tetrahedron Lett. 52 (2012) 5023–5026.
[16] K. Shinozuka, Y. Nakashima, K. Shimizu, H. Sawai, Synthesis and characterization of polyamine-based biomimetic catalysts as artificial ribonuclease, Nucleosides Nucleotides Nucleic Acids 20 (2001) 117–130.
[17] K. Shinozuka, K. Shimizu, Y. Nakashima, H. Sawai, Synthesis and RNA cleaving activities of polyamine derived novel artificial ribonuclease, Bioorg. Med. Chem. Lett. 4 (1994) 1979–1982.
[18] E. Delort, N.-Q. Nguyen-Trung, T. Darbre, J.-L. Reymond, Synthesis and activity of histidine-containing catalytic peptide dendrimers, J. Org. Chem. 71 (2006) 4468–4480.
[19] Y. Ma, X. Chen, M. Sun, R. Wan, C. Zhu, Y. Li, Y. Zhao, DNA cleavage function of seryl-histidine dipeptide and its application, Amino Acids 35 (2008) 251–256.
[20] P.Y. Ge, W. Zhao, Y. Du, J.J. Xu, H.Y. Chen, A novel hemin-based organic phase artificial enzyme electrode and its application in different hydrophobicity organic solvent, Biosens. Bioelectron. 24 (2009) 2002–2007.
[21] J.C. Verheijen, B.A.L.M. Deiman, E. Yeheskiely, G.A. van der Marel, J.H. van Boom, Efficient hydrolysis of RNA by a PNA–diethylenetriamine adduct, Angew. Chem. Int. Ed. 39 (2000) 369–372.
[22] T. Niittymäki, U. Kaukinen, P. Virta, S. Mikkola, H. Lönnberg, Preparation of azacrown-functionalized 2′-*O*-methyl oligoribonucleotides, potential artificial RNases, Bioconjug. Chem. 15 (2004) 174–184.
[23] N.G. Beloglazova, V.N. Sil'nikov, M.A. Zenkova, V.V. Vlassov, Cleavage of yeast tRNAPhe with complementary oligonucleotide conjugated to a small ribonuclease mimic, FEBS Lett. 481 (2000) 277–280.
[24] K. Ushijima, H. Gouzu, K. Hosono, M. Shirakawa, K. Kagosima, K. Takai, H. Takaku, Site-specific cleavage of tRNA by imidazole and/or primary amine groups bound at the 5′-end of oligodeoxyribonucleotides, Biochim. Biophys. Acta 1379 (1998) 217–223.
[25] C. Gnaccarini, S. Peter, U. Scheffer, S. Vonhoff, S. Klussmann, M.W. Göbel, Site-specific cleavage of RNA by a metal-free artificial nuclease attached to antisense oligonucleotides, J. Am. Chem. Soc. 128 (2006) 8063–8067.
[26] Y. Shao, X. Sheng, Y. Li, Z.L. Jia, J.J. Zhang, F. Liu, G.Y. Lu, DNA binding and cleaving activity of the new cleft molecule *N*, *N*′-bis(guanidinoethyl)-2,6-

pyridinedicarboxamide in the absence or in the presence of copper(II), Bioconjug. Chem. 19 (2008) 1840–1848.

[27] I. Szilágyi, O. Berkesi, M. Sipiczki, L. Korecz, A. Rockenbauer, I. Pálinkó, Preparation, characterization and catalytic activities of immobilized enzyme mimics, Catal. Lett. 127 (2009) 239–247.

[28] C.A. Deakyne, L.C. Allen, Role of active-site residues in the catalytic mechanism of ribonuclease A, J. Am. Chem. Soc. 101 (1979) 3951–3959.

[29] V.V. Vlassov, G. Zuber, B. Felden, J.-P. Behr, R. Giegé, Cleavage of tRNA with imidazole and spermine imidazole constructs: a new approach for probing RNA structure, Nucleic Acids Res. 23 (1995) 3161–3167.

[30] R. Breslow, How do imidazole groups catalyze the cleavage of RNA in enzyme models and in enzymes? Evidence from "negative catalysis", Acc. Chem. Res. 24 (1991) 317–324.

[31] J.H. Eastberg, J. Eklund, R. Monnat Jr., B.L. Stoddard, Mutability of an HNH nuclease imidazole general base and exchange of a deprotonation mechanism, Biochemistry 46 (2007) 7215–7225.

[32] T. Niittymäki, H. Lönnberg, Artificial ribonucleases, Org. Biomol. Chem. 4 (2006) 15–25.

[33] M.A. Catry, A. Madder, Synthesis of functionalized nucleosides for incorporation into nucleic acid-based serine protease mimics, Molecules 12 (2007) 114–129.

[34] Y. Bai, Y.B. Ling, W.G. Shi, L.F. Cai, Q.Y. Jia, S.B. Jiang, K.L. Liu, Heteromeric assembled polypeptidic artificial hydrolases with a six-helical bundle scaffold, ChemBioChem 12 (2011) 2647–2658.

[35] S.C. Holmes, M.J. Gait, Syntheses and oligonucleotide incorporation of nucleoside analogues containing pendant imidazolyl or amino functionalities – the search for sequence-specific artificial ribonucleases, Eur. J. Org. Chem. (2005) 5171–5183.

[36] D.A. Case, T.A. Darden, T.E. Cheatham, C.I. Simmerling, J. Wang, R.E. Duke, R. Luo, K.M. Merz, B. Wang, D.A. Peralman, M. Crowley, S. Brozell, V. Tsui, H. Gohlke, J. Mongan, V. Hornak, G. Cui, P. Beroza, C. Schafmeister, J.W. Caldwell, W.S. Ross, P.A. Kollma, Amber 8, University of California, San Francisco, USA, 2004.